

A FAST AND ROBUST NUMERICAL SOLUTION FOR THE POSITIONING DESIGN OF HORIZONTAL DRAINS IN A SATURATED-UNSATURATED SOIL GROUND SYSTEM

Qian HE*, Quan YUAN, Lin LANG

School of Architecture and Civil Engineering, Xihua University, Chengdu, China

*corresponding author, qianhxhu@163.com

This paper proposes an implicit difference solution to design the position of the horizontal drain in a saturated-unsaturated soil ground system (SUSGS). A complete system of classic diffusion equations is used to describe the transient flow of air and water phases in the soil system. Consolidation equations and boundary conditions are discretized by using the Crack–Nicolson (C-N) and virtual grid methods, respectively. The numerical scheme has been verified to be unconditionally stable based on von Neumann’s theorem. The comparison with existing analytical predictions confirms that the proposed solution is effective and accurate. According to the verified numerical solution, the optimum position of horizontal drains is designed to elevate the consolidation rate of the saturated-unsaturated soil ground system.

Keywords: consolidation; implicit difference solution; horizontal drain; saturated-unsaturated system; virtual grid method.



Articles in JTAM are published under Creative Commons Attribution 4.0 International.
Unported License <https://creativecommons.org/licenses/by/4.0/deed.en>.
By submitting an article for publication, the authors consent to the grant of the said license.

1. Introduction

In nature, the soil above and below the groundwater level exhibits unsaturated and saturated states, which forms a saturated-unsaturated soil ground system (SUSGS) (Li *et al.*, 2021). Due to the infiltration of rainfall, transpiration of plants, and extraction of groundwater, the soil system will change with the phreatic line. The decline or rise of groundwater may lead to building crack and non-uniform settlement of grounds. Therefore, some engineering requirements have been proposed to accelerate the discharge of the water phase. For instance, the horizontal drain is widely used in the construction of large airports (Mesri & Funk, 2015), highways (Zhou *et al.*, 2023), and railways (Gu *et al.*, 2020) to accelerate the drainage consolidation and improve the bearing capacity of the ground. The horizontal drain is placed between soil layers to shorten the seepage path of fluid and increase the consolidation rate of soil ground (Gibson & Shefford, 1968; Zhou *et al.*, 2024). Thus, it is meaningful to preliminarily assess the consolidation behavior of the SUSGS with horizontal drains.

Using the saturated soil model alone in geological engineering to solve drainage consolidation problems is convenient. Classical consolidation theory established by Terzaghi (1943) was applied to predict the consolidation behavior of the saturated soil. Some extended models are intended for the actual engineering problems, such as the ground with the horizontal drain (Feng *et al.*, 2019), layered soil (Feng *et al.*, 2020), and non-Darcy flow (Wu *et al.*, 2023). Based on Terzaghi’s theory and the engineering practice, a series of engineering technologies have been proposed to enhance the consolidation rate of soil ground. The horizontal drain is embedded at equal intervals in the soil layers to accelerate the consolidation rate in some geotechnical engineering (Lee *et al.*, 1987; Mesri & Funk, 2015). Meng *et al.* (2019), Li *et al.* (2020), and Feng *et al.* (2020) investigated the consolidation behavior of single-layer, double-layer, and four-layer saturated

ground with the horizontal drains. They provided constructive design schemes for the horizontal drain under different soil parameters.

For the consolidation of unsaturated soil, two typical diffusion equations for the air and water phases were obtained by Fredlund and Hasan (1979), which was used to estimate the dissipation of excess pore pressures and settlement of unsaturated soil. This original model and its extended form have been applied in various geotechnical engineering issues (Wang *et al.*, 2019; Yuan *et al.*, 2023; He *et al.*, 2025). The consolidation of unsaturated soil with horizontal drains needs more consideration. Zhou *et al.* (2023; 2024) proposed a semi-analytical solution to predict the consolidation behavior of double-layer unsaturated soil ground and a double-layer saturated-unsaturated soil ground system with the horizontal drain. However, in Zhou's literature, the horizontal drain is located at the interface between the upper and lower soil layers, and the position of the horizontal drain is not improved to be the best for discharging water. It is important to notice that the explicit difference method is employed to verify the correctness of analytical or semi-analytical solutions for the positioning design of horizontal drains in the SUSGS (Qin *et al.*, 2008; Wang *et al.*, 2017; 2019). With conditional stability and slow convergence, this difference scheme will cause high computational costs and poor reliability in solving consolidation problems.

The study reported in this paper attempts to develop an implicit difference solution with high computational efficiency and accuracy to design the position of horizontal drains in the SUSGS. The diffusion equations and boundary conditions are discretized using the Crack–Nicolson (C-N) and virtual grid methods. Then, the distribution of excess pore-air and pore-water pressures is obtained through matrix operation. Comparisons with the existing solutions are performed to verify the reliability and effectiveness of the numerical solution. Based on the proposed solution, the influence of horizontal drains on the SUSGS has been investigated, and the optimizing design of depths of horizontal drains is provided.

2. Mathematical model

2.1. Model description and basic assumptions

Combining the consolidation theories of the saturated and unsaturated soils proposed by Terzaghi (1943) and Fredlund *et al.* (2012), a simple mathematical description of the consolidation behavior of the SUSGS with horizontal drains is shown in Fig. 1. The SUSGS is divided into four zones by the embedment of two horizontal drains and an interface. Zone I comprises unsat-

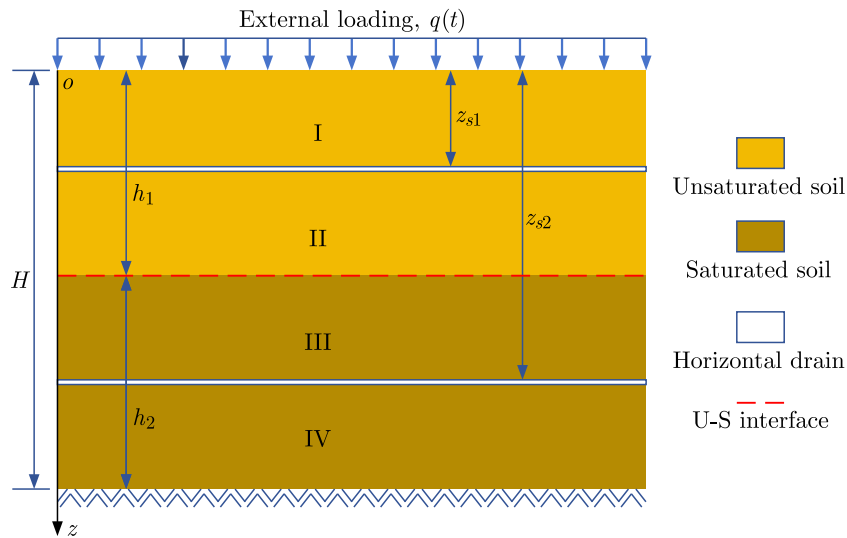


Fig. 1. Schematic diagram of SUSGS with horizontal drains.

urated soil with a two-way drainage system; the top and lower surfaces are permeable to air and water. In zone II, the upper surface is permeable to air and water phases, and the lower surface is impermeable to the air phase. Zone III is composed of saturated soil with a two-way drainage system. Zone IV has a one-way drainage system; the upper surface is permeable to water, and the bottom surface is impermeable. In the ground system, the thicknesses of the unsaturated and saturated soils are h_1 and h_2 , respectively, $h_1 + h_2 = H$; z_{s1} and z_{s2} are the imbedded depths of the first and second horizontal drains, respectively.

The main assumptions of the consolidation model for the SUSGS are as follows (Li *et al.*, 2021): (1) the unsaturated soil layer and saturated soil layer are both homogeneous; (2) the soil particles, water phase and horizontal drain are incompressible; (3) the flow of air and water phases along z -direction are independent, linear, and continuous steady-state; (4) in the consolidation process, the consolidation parameters keep constant; (5) the thickness of the capillary water zone is very thin, and its impact on the hydraulic response of the SUSGS is not significant.

It is worth noting that the above assumptions are not exact for all situations. For example, the soil is not homogeneous; it is composed of particles of different sizes and air and water. The influence of the capillary water zone on soils may be very significant. If we consider all these real situations, analyzing the consolidation behavior of such a complex system is far beyond our capability. In order to simplify the mathematical derivation process and preliminarily predict the consolidation behavior of the SUSGS, these listed assumptions are essential for developing the analytical and numerical solutions for the consolidation equations (Moradi *et al.*, 2019; Yuan *et al.*, 2023).

2.2. Consolidation equations

The volume changes associated with the water and air phases during the consolidation process can be calculated using Darcy's and Fick's laws. Then, the volume changes of the soil unit are equal to the sum of the volume changes of the air and water, and the governing equations are obtained (Li *et al.*, 2022):

$$\mathbf{C} \frac{\partial \mathbf{u}}{\partial t} + \mathbf{Z} \frac{\partial^2 \mathbf{u}}{\partial z^2} = \frac{\partial \mathbf{q}}{\partial t}, \quad (0 < z < h_1), \quad (2.1)$$

$$\frac{\partial u_v}{\partial t} + c_{vz} \frac{\partial^2 u_v}{\partial z^2} = \frac{\partial q}{\partial t}, \quad (h_1 < z < H), \quad (2.2)$$

where

$$\mathbf{u} = \begin{bmatrix} u_a \\ u_w \end{bmatrix}, \quad \mathbf{C} = \begin{pmatrix} 1 & c_a \\ c_w & 1 \end{pmatrix}, \quad \mathbf{Z} = \begin{pmatrix} c_{vz}^a & 0 \\ 0 & c_{vz}^w \end{pmatrix}, \quad \mathbf{q} = \begin{bmatrix} c_\sigma^a \\ c_\sigma^w \end{bmatrix} q(t),$$

u_a and u_w represent excess pore-air and pore-water pressures of unsaturated soil, respectively, u_w is excess pore-water pressure of saturated soil. In Eq. (2.1), c_a , c_{vz}^a , and c_σ^a are consolidation parameters of the air phase, c_w , c_{vz}^w , and c_σ^w are consolidation parameters of the water phase. In Eq. (2.2), c_{vz} is consolidation parameters of the saturated soil. The definitions and expressions of these consolidation parameters can be found in (Fredlund, 2012; Terzaghi, 1943).

2.3. Model conditions

The drainage conditions of the SUSGS are:

– for zone I

$$\mathbf{u}(0, t) = \mathbf{0}, \quad (2.3)$$

$$\mathbf{u}(z_{s1}, t) = \mathbf{0}, \quad (2.4)$$

– for zone II

$$\mathbf{u}(z_{s1}, t) = \mathbf{0}, \quad (2.5)$$

$$\frac{\partial u_a(h_1, t)}{\partial z} = 0, \quad (2.6)$$

$$k_w \frac{\partial u_w(h_1, t)}{\partial z} = k_v \frac{\partial u_v(h_1, t)}{\partial z}, \quad u_w(h_1, t) = u_v(h_1, t), \quad (2.7)$$

– for zone III

$$k_w \frac{\partial u_w(h_1, t)}{\partial z} = k_v \frac{\partial u_v(h_1, t)}{\partial z}, \quad u_w(h_1, t) = u_v(h_1, t) \quad (2.8)$$

$$u_v(z_{s2}, t) = 0, \quad (2.9)$$

– for zone IV

$$u_v(z_{s2}, t) = 0, \quad (2.10)$$

$$\frac{\partial u_v(H, t)}{\partial z} = 0. \quad (2.11)$$

The initial conditions are expressed as

$$\mathbf{u}(z, 0) = f(z) [u_a^0 \ u_w^0]^\top, \quad (0 < z \leq h_1), \quad (2.12)$$

$$u_v(z, 0) = f(z)p_0, \quad (h_1 < z < H), \quad (2.13)$$

where u_a^0 , u_w^0 , and p_0 are initial excess pore pressures at $t = 0$; $f(z)$ is a distribution function about z .

3. Solution derivation

3.1. Crack–Nicolson (C-N) solution for consolidation equations

The C-N method has been widely used to solve a single Navier-Stokes equation (Feng *et al.*, 2020). For a system of partial differential equations containing three variables (u_a , u_w , and u_v) and a series of definite solution conditions (Eqs. (2.3)–(2.13)), some technical improvements are needed when using the C-N method to solve it. The difference mesh for the SUSGS is shown in Fig. 2. The time and spatial domains are divided into N and K equidistant nodes, respectively. Time step and space step are τ and h . The node coordinates are (z_k, t_n) , and $z_k = kh_z$, $k = 0, 1, 2, \dots, K$; $t_n = n\tau$, $n = 0, 1, 2, \dots, N$. z_{k1} and z_{k2} represent the positions of the first and second horizontal drains, respectively, where $z_0 < z_{k1}$, $z_{k2} < z_K$. z_M denotes the U-S interface.

Equations (2.1) and (2.2) can be discretized as

$$\mathbf{C} \frac{\mathbf{u}_k^{n+1} - \mathbf{u}_k^n}{\tau} + \mathbf{Z} \frac{\delta_z^2 \mathbf{u}_k^{n+1} + \delta_z^2 \mathbf{u}_k^n}{2h_z^2} = \frac{\mathbf{q}^{n+1} - \mathbf{q}^n}{\tau}, \quad (1 \leq j \leq M-1), \quad (3.1)$$

$$\frac{u_{vk}^{n+1} - u_{vk}^n}{\tau} + c_{vz} \frac{\delta_z^2 u_{vk}^{n+1} + \delta_z^2 u_{vk}^n}{2h_z^2} = \frac{q^{n+1} - q^n}{\tau}, \quad (M+1 \leq j \leq K-1), \quad (3.2)$$

where $\delta_z^2 \mathbf{u}_j^n = \mathbf{u}_{k-1}^n - 2\mathbf{u}_k^n + \mathbf{u}_{k+1}^n$, $\delta_z^2 u_{vk}^n = u_{v(k-1)}^n - 2u_{vk}^n + u_{v(k+1)}^n$.

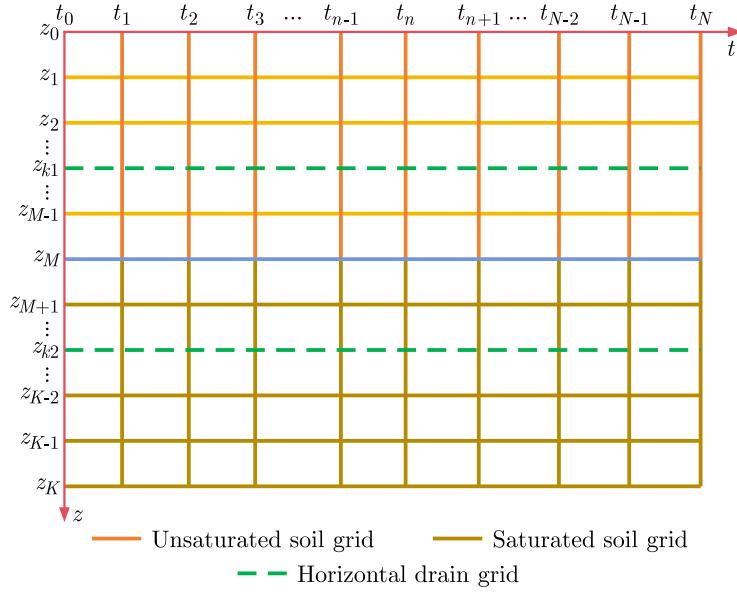


Fig. 2. C-N scheme for difference grid of the saturated-unsaturated soil system ground.

Equations (3.1) and (3.2) can be rewritten as

$$\begin{aligned} \frac{1}{2}\lambda_z \mathbf{Z} \mathbf{u}_{k-1}^{n+1} + (\mathbf{C} - \lambda_z \mathbf{Z}) \mathbf{u}_k^{n+1} + \frac{1}{2}\lambda_z \mathbf{Z} \mathbf{u}_{k+1}^{n+1} = & -\frac{1}{2}\lambda_z \mathbf{Z} \mathbf{u}_{k-1}^n \\ & + (\mathbf{C} + \lambda_z \mathbf{Z}) \mathbf{u}_k^n - \frac{1}{2}\lambda_z \mathbf{X} \mathbf{u}_{k-1}^n + \mathbf{q}^{n+1} - \mathbf{q}^n, \end{aligned} \quad (3.3)$$

$$\begin{aligned} \frac{1}{2}\lambda_z c_{vz} u_{v(k-1)}^{n+1} + (1 - \lambda_z c_{vz}) u_{vk}^{n+1} + \frac{1}{2}\lambda_z c_{vz} u_{v(k+1)}^{n+1} = & -\frac{1}{2}\lambda_z c_{vz} u_{v(k-1)}^n \\ & + (1 + \lambda_z c_{vz}) u_{vk}^n - \frac{1}{2}\lambda_z c_{vz} u_{v(k+1)}^n + q^{n+1} - q^n, \end{aligned} \quad (3.4)$$

where $\lambda_z = \tau/h^2$.

Equations (3.3) and (3.4) contain three unknown quantities and three known quantities on adjacent layer k . The value of mesh nodes can only be obtained by using the matrix operation. Equations (3.3) and (3.4) are written as

$$\mathbf{A}_u \mathbf{D}_u^{n+1} = \mathbf{B}_u \mathbf{D}_u^n + \mathbf{Q}_u^n, \quad (1 \leq j \leq M-1), \quad (3.5)$$

$$\mathbf{A}_s \mathbf{D}_s^{n+1} = \mathbf{B}_s \mathbf{D}_s^n + \mathbf{Q}_s^n, \quad (M+1 \leq j \leq K-1), \quad (3.6)$$

where \mathbf{A}_u and \mathbf{B}_u are coefficient matrices, \mathbf{Q}_u^n and \mathbf{Q}_s^n are composed of the external loading, \mathbf{D}_u^n and \mathbf{D}_s^n are composed of the pore-air and pore-water pressures. The specific expressions of these parameters are shown in Appendix A.

It is necessary to validate the stability and convergence of the proposed difference method, which can be verified using von Neumann's theorem (Sharifi & Rashidinia, 2016). The derivation of stability is shown in Appendix B.

3.2. Boundary conditions discretization

The permeable boundary conditions, Eqs. (2.3)–(2.5), (2.9), and (2.10), are regarded as known quantities appearing on the right-hand sides of Eqs. (3.3) and (3.4). If the interface ($z = h_1$ and $z = H$) satisfies the impermeable and continuous permeable boundaries, we use the

virtual mesh method (Morton & Mayers, 2005) to obtain the discrete scheme of Eqs. (2.6)–(2.8), and (2.11).

As shown in Figs. 3a and 3b, the virtual layers of the air and water pressures are constructed outside the boundary. Then, Eqs. (2.6) and (2.11) are discretized by the central difference:

$$\frac{u_{v(K+1)}^n - u_{v(K-1)}^n}{2h_z} = 0, \quad (3.7)$$

$$\frac{u_{a(M+1)}^n - u_{a(M-1)}^n}{2h_z} = 0. \quad (3.8)$$

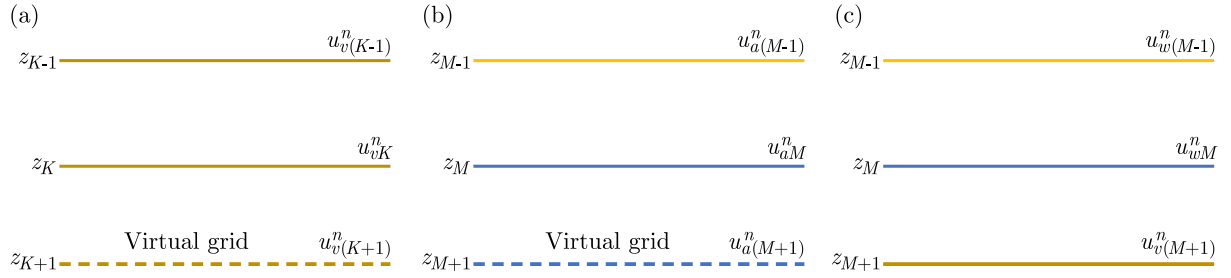


Fig. 3. Difference mesh at the boundary: (a) $z = z_K$; (b) z_M for air phase; (c) z_M for water phase.

Substituting Eqs. (3.7) and (3.8) into Eqs. (3.3) and (3.4) to eliminate the virtual nodes, the difference format at the impermeable boundary is obtained.

The forward and backward difference quotients are used to discretize the left and right sides of Eq. (2.8):

$$k_w \frac{u_{wM}^n - u_{w(M-1)}^n}{h} = k_v \frac{u_{vM}^n - u_{v(M+1)}^n}{h}, \quad (3.9)$$

$$u_{wM}^n = u_{vM}^n. \quad (3.10)$$

As shown in Fig. 3c, the difference scheme of Eq. (3.3) at $z = z_M$ includes the nodes $u_{w(M-1)}^n$, u_{wM}^n , and $u_{v(M+1)}^n$, so it is represented as

$$\begin{aligned} \frac{1}{2}\lambda_z c_{vz}^w u_{w(M-1)}^{n+1} + (1 - \lambda_z c_{vz}^w) u_{wM}^{n+1} + \frac{1}{2}\lambda_z c_{vz} u_{v(M+1)}^{n+1} + c_w u_{a(M-1)}^{n+1} = & -\frac{1}{2}\lambda_z c_{vz}^w u_{w(M-1)}^n \\ & + (1 + \lambda_z c_{vz}^w) u_{wM}^n - \frac{1}{2}\lambda_z c_{vz} u_{v(M+1)}^n + c_w u_{a(M-1)}^n + c_\sigma^w (q^{n+1} - q^n). \end{aligned} \quad (3.11)$$

In the above equation, $u_{v(M+1)}^{n+1}$ and $u_{v(M+1)}^n$ are the virtual nodes. The difference solution of Eq. (3.3) at $z = z_M$ is obtained by substituting Eq. (3.9) into Eq. (3.11) to eliminate these virtual nodes.

Similarly, the difference solution of Eq. (3.4) at $z = z_M$ contains the nodes $u_{w(M-1)}^n$, u_{vM}^n , and $u_{v(M+1)}^n$ in the iteration process. The difference scheme is expressed as follows:

$$\begin{aligned} \frac{1}{2}\lambda_z c_{vz}^w u_{w(M-1)}^{n+1} + (1 - \lambda_z c_{vz}^w) u_{vM}^{n+1} + \frac{1}{2}\lambda_z c_{vz} u_{v(M+1)}^{n+1} = & -\frac{1}{2}\lambda_z c_{vz}^w u_{w(M-1)}^n \\ & + (1 + \lambda_z c_{vz}^w) u_{vM}^n - \frac{1}{2}\lambda_z c_{vz} u_{v(M+1)}^n + q^{n+1} - q^n, \end{aligned} \quad (3.12)$$

where $u_{w(M-1)}^{n+1}$ and $u_{w(M-1)}^n$ are the virtual nodes.

Substituting Eq. (3.9) into Eq. (3.12) to eliminate these virtual nodes, the C-N solution for Eq. (3.4) at $z = z_M$ can be obtained. Adding the difference scheme of Eqs. (3.3) and (3.4) at $z = z_M$, the C-N solution at the interface ($z = h_1$) is

$$\begin{aligned} \alpha_{M-1}u_{w(M-1)}^{n+1} + \alpha_M u_{wM}^{n+1} + \alpha_{M+1}u_{v(M+1)}^{n+1} + c_w u_{a(M-1)}^{n+1} &= \beta_{M-1}u_{w(M-1)}^n \\ &+ \beta_M u_{wM}^n + \beta_{M+1}u_{v(M+1)}^n + c_w u_{a(M-1)}^n + (c_\sigma^w + 1)(q^{n+1} - q^{n-1}), \end{aligned} \quad (3.13)$$

where $\alpha_{m-1}, \dots, \gamma_{m+1}$ are constant coefficients.

In the above derivation, we give the difference schemes of the consolidation equations and boundary conditions. The final C-N solution can be expressed as

$$\mathbf{A}\mathbf{D}^{n+1} = \mathbf{B}\mathbf{D}^n + \mathbf{Q}^n, \quad (3.14)$$

where \mathbf{A} and \mathbf{B} are partitioned matrices. Their description can be found in Appendix C.

3.3. Settlement discretization

Based on generalized Hooke's law, the volume change of soil structure can be formulated by the net normal stress and matrix suction. After obtaining the excess pore pressures by using Eq. (3.14), the volumetric strain of the unsaturated soil is expressed as (Fredlund *et al.*, 2012):

$$d\varepsilon_{wk}^n = m_1^s d(q^n - u_{ak}^n) + m_2^s d(u_{ak}^n - u_{wk}^n), \quad (3.15)$$

where m_1^s and m_2^s are the coefficients of soil volume changes with respect to the net normal stress and matrix suction.

The volumetric strain of the saturated soil is expressed as

$$d\varepsilon_{vk}^n = m_v d(q^n - u_{vk}^n). \quad (3.16)$$

The settlement of the SUSGS is

$$S(t_n) = h_z \left(\sum_{k=0}^M \varepsilon_{wk}^n + \sum_{k=M+1}^K \varepsilon_{vk}^n \right). \quad (3.17)$$

The average degree of consolidation is

$$S^* = \frac{S(t_n)}{S(t_\infty)} \times 100\%, \quad (3.18)$$

where $S(t_\infty)$ is the maximum settlement of the SUSGS.

4. Verification

In order to verify the convergence (effectiveness and reliability) of the C-N solution, a comparison of the numerical results and analytical solution (Zhou *et al.*, 2023) is made. The consolidation parameters are assumed as follows: $c_a = -0.0899$, $c_w = 0.75$, $c_{vx}^a = -5.3476 \times 10^{-6} \text{ m/s}^2$, $c_{vz}^w = -5.108 \times 10^{-8} \text{ m/s}^2$, $u_a^0 = 20 \text{ kPa}$, $u_w^0 = 40 \text{ kPa}$, $c_{vz} = -8.16310^{-7} \text{ m/s}^2$, $p_0 = 100 \text{ kPa}$, $H = 10 \text{ m}$, $h_1 = 5 \text{ m}$, $q(t) = 100 \text{ kPa}$. Figure 4 shows the distribution of pore pressures in the SUSGS with one horizontal drain ($t = 10^5 \text{ s}$ for air phase, and $t = 10^7 \text{ s}$ for water phase). The proposed numerical solution agrees with the analytical solutions, suggesting that it is reliable and accurate. Further validation for the computational efficiency of the proposed algorithm under different grid ratios is given in Appendix D.

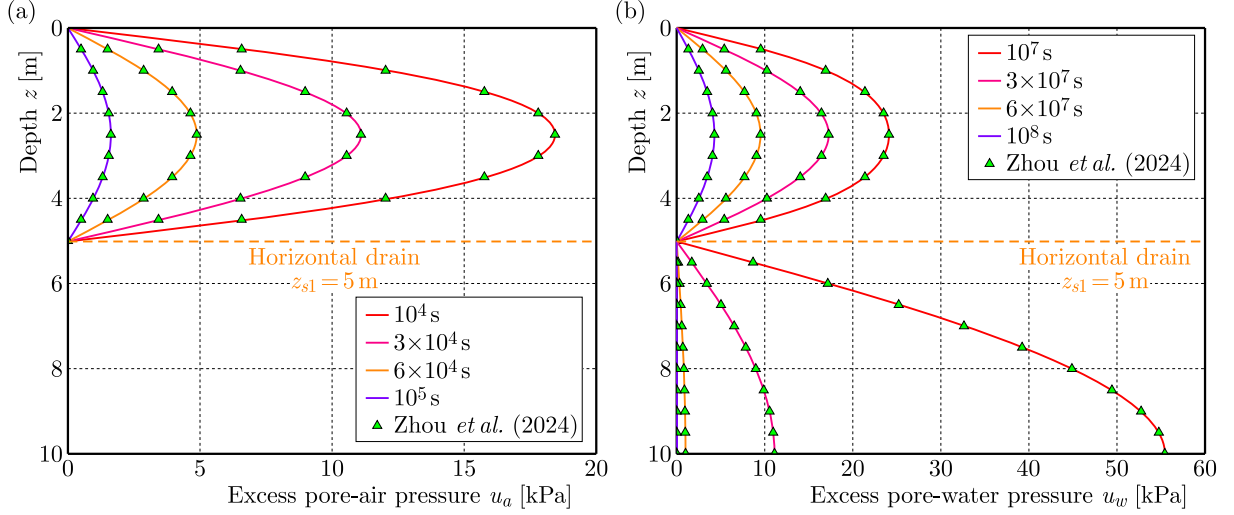


Fig. 4. Distribution of excess pore pressures along the depth direction: (a) u_a and (b) u_w .

5. Numerical examples

5.1. The position design of a single horizontal drain

The purpose of installing the horizontal drain is to accelerate the consolidation rate of the ground. The optimal position for the horizontal drain is to achieve the consolidation degree of 90 % in the shortest time (Meng *et al.*, 2019). Hence, the objective function can be expressed as

$$\min T_v = T_{90}(z_{s1}), \quad (5.1)$$

where T_v is the objective function, T_{90} is the time cost for consolidation degree of 90 %.

Based on Eq. (3.18), the relationship between the embedded depth of the horizontal drain and the time costs is plotted in Fig. 5. The influence of different phreatic lines (see Table 1) on the position design of the horizontal drain is considered. Compared with the traditional design scheme (Wang *et al.*, 2017; Lei *et al.*, 2016), the horizontal drain at the optimal position can further shorten the consolidation time. A large h_1 will cause the optimal position to move downwards; conversely, the optimal position will move upwards as h_1 decreases. The consolidation rate of the SUSGS with the sand blanket at the optimal position significantly increased (20–80 times) compared to that without the horizontal drain, implying that the horizontal drain shortens the consolidation time and improves engineering efficiency (Zhou *et al.*, 2024).

Table 1. Thickness of unsaturated and saturated soils under different case conditions.

Case	h_1 [m]	h_2 [m]
1	3	7
2	5	5
3	7	3

5.2. The position design of two horizontal drains

If the two horizontal drains are embedded in the SUSGS, the objective function is

$$\min T_v = T_{90}(z_{s1}, z_{s2}). \quad (5.2)$$

Figure 6 shows the distribution of time costs under different depths z_{s1} and z_{s2} , under the condition of $S^* = 90$ %. By comparing Figs. 5 and 6, the two horizontal drains further accelerate

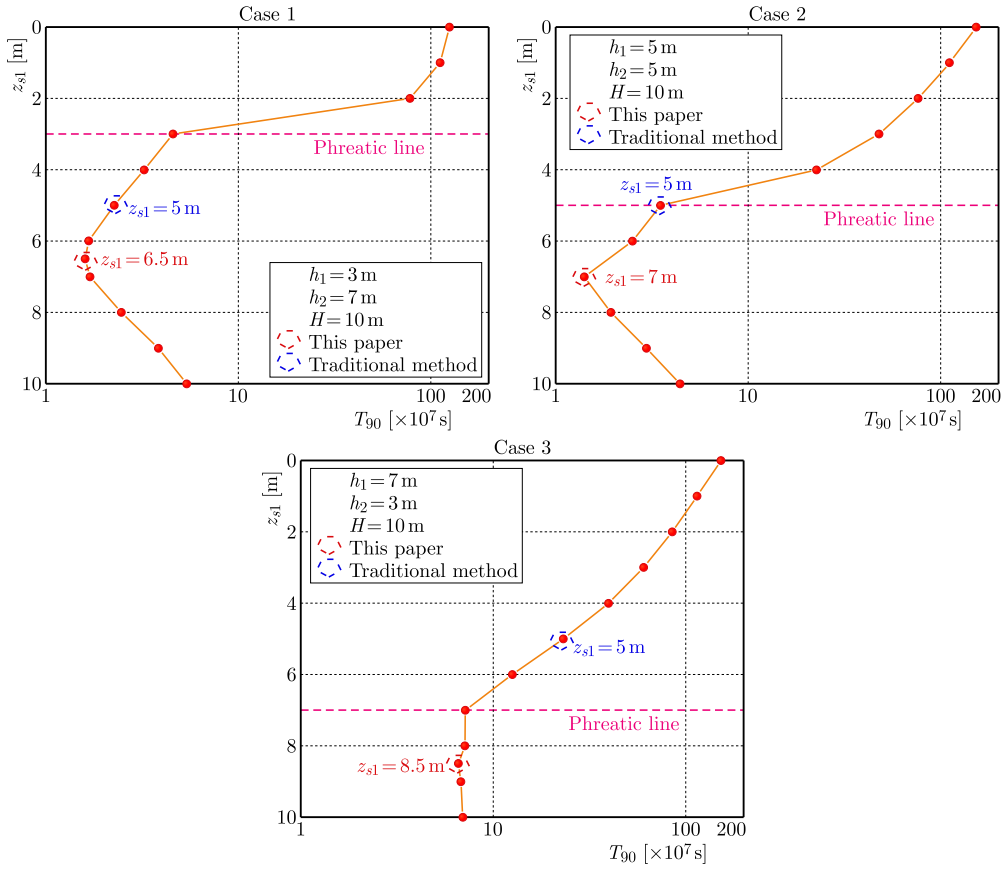


Fig. 5. Relationship between the embedded depth of the horizontal drain and the time costs when $S^* = 90\%$.

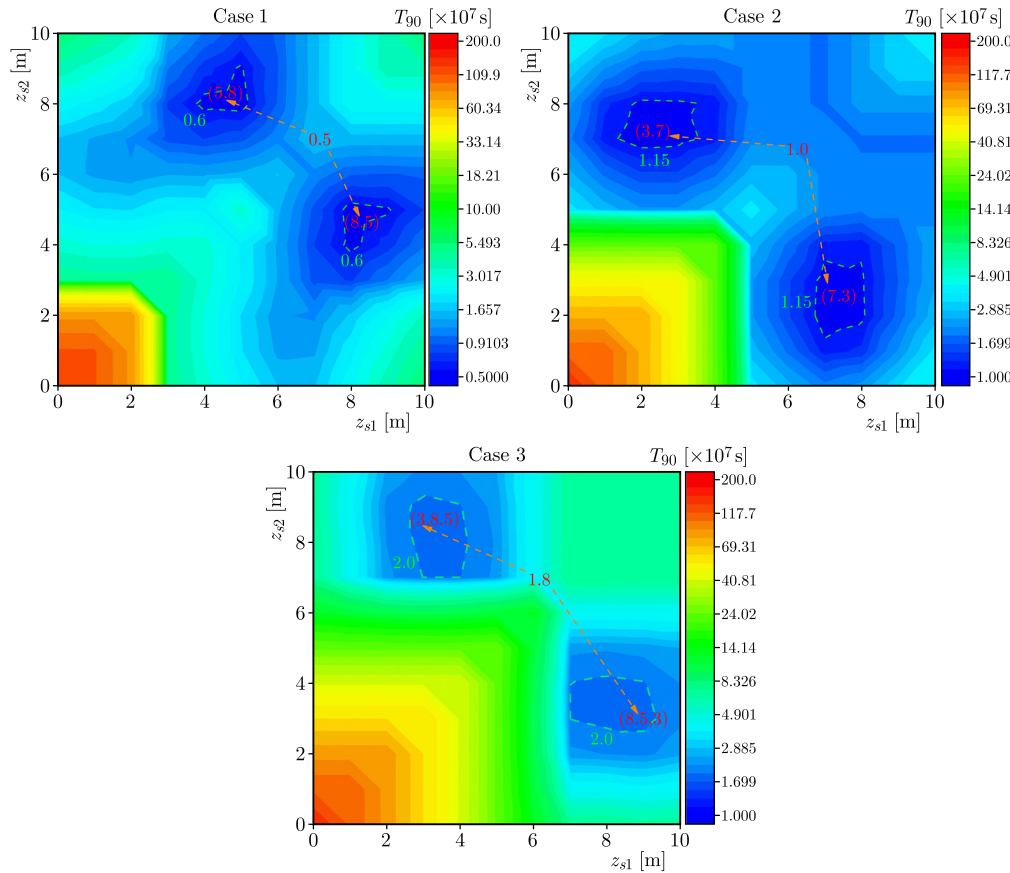


Fig. 6. Time distribution of different depth z_{s1} and z_{s2} when S_{90} .

the consolidation rate. In case 1, the smaller time region (green dashed line) can be found if the horizontal drains are located in the saturated soil layer. The smaller the proportion of unsaturated soil, the more the discharge of excess pore-water pressure in the saturated soil is clogged at the saturated-unsaturated interface. Therefore, there is no need to place a horizontal drain in the unsaturated soil layer. In cases 2 and 3, only when the two horizontal drains are placed in different soil layers, the optimal position of drains in the SUSGS denoted by the smaller time region is obtained. In addition, the larger the proportion of unsaturated soil (i.e., the larger h_1), the slower the consolidation rate of the SUSGS. The consolidation rate of the SUSGS with two horizontal drains is increased 100–150 times compared to that without the horizontal drain. According to the proposed solution's convenience, the optimal position of the horizontal drains in practical engineering can be preliminarily designed.

Table 2 shows the consolidation time considering the traditional design scheme and the proposed optimal position. The horizontal drains are placed at equal intervals in the traditional design scheme. It is found that T_{90} under the traditional design scheme is larger than that under the optimal scheme. If three horizontal drains are located in the SUSGS, the shortest consolidation time is spent. But it may need more engineering resources. A more reasonable choice is to arrange two horizontal drains in the SUSGS. The scheme provided in this paper can achieve a balance between consolidation time and engineering resources.

Table 2. T_{90} (days) for different design schemes for the horizontal drain.

Case	Without horizontal drain	Number of horizontal drains				
		1	2	3	1	2
1	14 467	<i>262</i>	<i>163</i>	<i>60</i>	189	58
2	17 824	<i>406</i>	<i>176</i>	<i>88</i>	236	115
3	17 708	<i>2685</i>	<i>1140</i>	<i>113</i>	775	208

Note: Italicized numbers represent the consolidation time under traditional design schemes. Bold numbers denote the consolidation time under the design scheme of this article.

6. Conclusions

This paper proposes a numerical solution with high computational efficiency and accuracy for designing the position of the horizontal drains in the SUSGS. Based on the consolidation theories of the unsaturated and saturated soils, the two sets of diffusion equations are used to simulate the transient flow of air and water phases. Then, the diffusion equations are discretized by the C-N scheme to obtain the numerical solution for the SUSGS. The proposed numerical solution is reliable and accurate when compared with the analytical solution. According to the verified solution, the influence of the horizontal drains on the consolidation behavior of the SUSGS is investigated to design its optimal position. The results show that the arrangement of the horizontal drain can significantly accelerate the consolidation rate of the entire ground. The horizontal drain at the optimal position can save consolidation time and promote the consolidation speed.

Appendix A

$$\mathbf{A}_u = \begin{pmatrix} 1 - \lambda_z c_{vz}^a & c_a & 0.5\lambda_z c_{vz}^a & \cdots & 0 & 0 \\ c_w & 1 - \lambda_z c_{vz}^w & 0 & 0.5\lambda_z c_{vz}^w & & \\ 0.5\lambda_z c_{vz}^a & c_w & 1 - \lambda_z c_{vz}^a & & & \\ \vdots & \vdots & \vdots & \ddots & \vdots & \vdots \\ & & 0.5\lambda_z c_{vz}^a & 0 & 1 - \lambda_z c_{vz}^a & c_a \\ 0 & 0 & & 0.5\lambda_z c_{vz}^w & c_a & 1 - \lambda_z c_{vz}^w \end{pmatrix}, \quad (\text{A.1})$$

$$\mathbf{B}_u = \begin{pmatrix} 1 + \lambda_z c_{vz}^a & c_a & -0.5\lambda_z c_{vz}^a & \cdots & 0 & 0 \\ c_w & 1 + \lambda_z c_{vz}^w & 0 & -0.5\lambda_z c_{vz}^w & & \\ -0.5\lambda_z c_{vz}^a & c_w & 1 + \lambda_z c_{vz}^a & & & \\ \vdots & \vdots & \vdots & \ddots & \vdots & \vdots \\ & & -0.5\lambda_z c_{vz}^a & 0 & 1 + \lambda_z c_{vz}^a & c_a \\ 0 & 0 & & -0.5\lambda_z c_{vz}^w & c_w & 1 + \lambda_z c_{vz}^w \end{pmatrix}, \quad (\text{A.2})$$

$$\mathbf{A}_s = \begin{pmatrix} 1 - \lambda_z c_{vz} & 0.5\lambda_z c_{vz} & \cdots & 0 & 0 \\ 0.5\lambda_z c_{vz} & 1 - \lambda_z c_{vz} & & & \\ \vdots & \vdots & \ddots & \vdots & \vdots \\ & & & 1 - \lambda_z c_{vz} & 0.5\lambda_z c_{vz} \\ 0 & 0 & \cdots & 0.5\lambda_z c_{vz} & 1 - \lambda_z c_{vz} \end{pmatrix}, \quad (\text{A.3})$$

$$\mathbf{B}_s = \begin{pmatrix} 1 + \lambda_z c_{vz} & -0.5\lambda_z c_{vz} & \cdots & 0 & 0 \\ -0.5\lambda_z c_{vz} & 1 + \lambda_z c_{vz} & & & \\ \vdots & \vdots & \ddots & \vdots & \vdots \\ & & & 1 + \lambda_z c_{vz} & -0.5\lambda_z c_{vz} \\ 0 & 0 & \cdots & -0.5\lambda_z c_{vz} & 1 + \lambda_z c_{vz} \end{pmatrix}, \quad (\text{A.4})$$

$$\mathbf{D}_u^n = \begin{bmatrix} u_{a1}^{(1)n} & u_{w1}^{(1)n} & \cdots & u_{a(M-1)}^{(1)n} & u_{w(M-1)}^{(1)n} \end{bmatrix}^T, \quad (\text{A.5})$$

$$\mathbf{D}_s^n = \begin{bmatrix} u_{w(M+1)}^{(2)n} & u_{w(M+2)}^{(2)n} & \cdots & u_{w(J-2)}^{(2)n} & u_{w(J-1)}^{(2)n} \end{bmatrix}^T, \quad (\text{A.6})$$

$$\mathbf{Q}_u^n = (q^{n+1} - q^n) \begin{bmatrix} c_\sigma^a & c_\sigma^w & \cdots & c_\sigma^a & c_\sigma^w \end{bmatrix}^T, \quad (\text{A.7})$$

$$\mathbf{Q}_s^n = (q^{n+1} - q^n) \begin{bmatrix} 1 & 1 & \cdots & 1 & 1 \end{bmatrix}^T, \quad (\text{A.8})$$

where \mathbf{A}_u and \mathbf{B}_u are five-diagonal sparse matrices, \mathbf{A}_s and \mathbf{B}_s are tridiagonal sparse matrices.

Appendix B

Derivation of stability

In the von Neumann criterion, a standardized trial solution is proposed to verify the stability of the difference scheme. The trial solution of Eq. (3.3) at point (z_k, t_n) is assumed to be:

$$\mathbf{u}_j^n = \mathbf{v}^n e^{ik\zeta h_z}, \quad (\text{B.1})$$

where $\mathbf{u}_k^n = [u_{ak}^n \ u_{wk}^n]^T$, $i^2 = -1$, ζ reflects the small errors caused by node j iterating in the adjacent time layers.

Substituting Eq. (B.1) into Eq. (3.3) yields:

$$\mathbf{G}_1 \mathbf{v}^{n+1} = \mathbf{G}_2 \mathbf{v}^n, \quad (\text{B.2})$$

where

$$\mathbf{G}_{u1} = \begin{pmatrix} 1 - 2\lambda_z \alpha c_{vz}^a & c_a \\ c_w & 1 - 2\lambda_z \alpha c_{vz}^w \end{pmatrix}, \quad \mathbf{G}_{u2} = \begin{pmatrix} 1 + 2\lambda_z \alpha c_{vz}^a & c_a \\ c_w & 1 + 2\lambda_z \alpha c_{vz}^w \end{pmatrix},$$

$$\alpha = \left(\sin \left(\frac{\zeta h}{2} \right) \right)^2.$$

The growth matrix of Eq. (3.3) is

$$\mathbf{G}_u = (\mathbf{G}_{u1})^{-1} \mathbf{G}_{u2}. \quad (\text{B.3})$$

Based on Eq. (B.3), the eigenvalues of the growth matrix are

$$\mu_1 = \frac{c_a c_w + 4a^2 \lambda_z^2 c_{vz}^a c_{vz}^w - 1 - 2a \lambda_z \left[(c_{vz}^a)^2 - 2c_{vz}^a c_{vz}^w + (c_{vz}^w)^2 + 4c_a c_w c_{vz}^a c_{vz}^w \right]^{1/2}}{c_a c_w - 4a^2 \lambda_z^2 c_{vz}^a c_{vz}^w - 1 + 2a \lambda_z c_{vz}^a + 2a \lambda_z c_{vz}^w}, \quad (\text{B.4})$$

$$\mu_2 = \frac{c_a c_w + 4a^2 \lambda_z^2 c_{vz}^a c_{vz}^w - 1 + 2a \lambda_z \left[(c_{vz}^a)^2 - 2c_{vz}^a c_{vz}^w + (c_{vz}^w)^2 + 4c_a c_w c_{vz}^a c_{vz}^w \right]^{1/2}}{c_a c_w - 4a^2 \lambda_z^2 c_{vz}^a c_{vz}^w - 1 + 2a \lambda_z c_{vz}^a + 2a \lambda_z c_{vz}^w}. \quad (\text{B.5})$$

According to the von Neumann criterion, the difference scheme is unconditionally stable only when all absolute values of eigenvalues ($|u_1 \sim u_2| \leq 1$) are less than or equal to 1. Otherwise, it is conditionally stable. Based on Eqs. (B.4) and (B.5), considering that the consolidation parameters (c_{vz}^a and c_{vz}^w) of soil are very small, the denominator is always greater than the numerator in the eigenvalues. Thus, the C-N scheme for the consolidation equations of the unsaturated soil is unconditionally stable under the arbitrary mesh ratio (λ_z).

Similarly, the trial solution of Eq. (3.4) at point (z_k, t_n) is assumed to be:

$$u_{wj}^{(2)n} = v_w^{(2)n} e^{ik\zeta h}. \quad (\text{B.6})$$

Substituting Eq. (B.6) into Eq. (3.4) yields:

$$G_{s1} v_w^{(2)n+1} = G_{s2} v_w^{(2)n}, \quad (\text{B.7})$$

where $G_{s1} = 1 - 2\lambda_z \alpha c_{vz}$, $G_{s2} = 1 + 2\lambda_z \alpha c_{vz}$.

The growth factor of Eq. (3.4) is:

$$G_s = G_{s2}/G_{s1} = \frac{1 + 2\lambda_z \alpha c_{vz}}{1 - 2\lambda_z \alpha c_{vz}}. \quad (\text{B.8})$$

It can be found that growth factor G_s is less than 1 under the arbitrary mesh ratio, so the C-N solution for the consolidation equation of the saturated soil is also unconditionally stable.

Appendix C

A and **B** are the partitioned matrices, and they are expressed as

$$\mathbf{A} = \begin{pmatrix} \text{blue} & \text{yellow} & \dots & \mathbf{0} & \dots & \mathbf{0} \\ \vdots & \text{green} & \text{yellow} & \text{red} & \text{orange} & \vdots \\ \mathbf{0} & \vdots & \text{red} & \text{orange} & \text{green} & \mathbf{0} \\ \vdots & \mathbf{0} & \vdots & \text{orange} & \text{green} & \vdots \\ \mathbf{0} & \dots & \mathbf{0} & \dots & \text{orange} & \text{blue} \end{pmatrix} \quad \begin{array}{ll} \text{blue} & \mathbf{A}_0, \mathbf{A}_J \\ \text{yellow} & \mathbf{A}_u \\ \text{red} & \mathbf{A}_M \\ \text{orange} & \mathbf{A}_s \\ \text{green} & \mathbf{A}_{k1}, \mathbf{A}_{k2} \end{array} \quad (\text{C.1})$$

where \mathbf{A}_0 and \mathbf{A}_J are the coefficient matrices of Eqs. (3.3) and (3.4) at the boundary $z = z_0$ and $z = z_J$, respectively, \mathbf{A}_M is coefficient matrices on the left side of Eq. (3.13), \mathbf{A}_{m1} and \mathbf{A}_{m2} are identity matrices:

$$\mathbf{B} = \begin{pmatrix} \text{blue} & \text{yellow} & \dots & \mathbf{0} & \dots & \mathbf{0} \\ \vdots & \text{green} & \text{yellow} & \vdots & \vdots & \vdots \\ \mathbf{0} & \vdots & \text{red} & \text{orange} & \text{green} & \vdots \\ \vdots & \vdots & \vdots & \vdots & \vdots & \vdots \\ \mathbf{0} & \dots & \mathbf{0} & \dots & \text{orange} & \text{blue} \\ \mathbf{0} & \vdots & \vdots & \vdots & \vdots & \vdots \end{pmatrix} \quad \begin{array}{l} \text{blue} \quad \mathbf{B}_0, \mathbf{B}_J \\ \text{yellow} \quad \mathbf{B}_u \\ \text{red} \quad \mathbf{B}_M \\ \text{orange} \quad \mathbf{B}_s \\ \text{green} \quad \mathbf{B}_{k1}, \mathbf{B}_{k2} \end{array} \quad (\text{C.2})$$

Appendix D

Comparison of computational efficiency and accuracy

As shown in Tables D1 and D2, the numerical solution developed in this paper has high computational efficiency and stability under the arbitrary mesh ratio condition. It is worth noting that the C-N scheme at the local region has been proven to be unconditionally stable. In order to verify the overall stability of the C-N solution, the boundary conditions, initial conditions, and external loading are considered in this example. It can be seen that the numerical solution also exhibits strong stability, indicating that the C-N solution can solve consolidation problems under various boundary conditions, initial conditions, and time-dependent loading.

Table D1. Comparison of the calculation results between the numerical and analytical solutions.

Time step τ [s]	Time costs [s]	Water pressure [kPa], $h_z = 1$ m, $t_n = 10^7$ s			
		$z = 1$ m	$z = 3$ m	$z = 5$ m	$z = 7$ m
10	258.25	20.33	32.64	86.04	90.13
100	24.32	20.33	32.64	86.04	90.13
1000	2.26	20.33	32.64	86.04	90.13
10 000	0.35	20.33	32.64	86.04	90.13
Yuan <i>et al.</i> (2023)	—	20.34	32.64	86.05	90.13

Note: $t_N = 10^9$ s

Table D2. Comparison of the calculation results between the numerical and analytical solutions.

Depth step h_z	Water pressure [kPa], $\tau = 100$ s, $t_n = 10^7$ s			
	$z = 1$ m	$z = 3$ m	$z = 5$ m	$z = 7$ m
0.1	20.33	32.64	86.04	90.13
0.2	20.33	32.64	86.04	90.13
0.25	20.33	32.64	86.04	90.13
0.5	20.33	32.64	86.04	90.13
1	20.33	32.64	86.04	90.13

Acknowledgments

The authors gratefully acknowledge the financial support for this work from the National Engineering Laboratory for Highway Tunnel Construction Technology (grant no. NELFHT201702), Natural Science Foundation of Sichuan (grant no. 2022NSFSC0443).

References

1. Feng, J.X., Ni, P.P., Chen, Z., Mei, G.X., & Xu, M.J. (2020). Positioning design of horizontal drain in sandwiched clay-drain systems for land reclamation. *Computers and Geotechnics*, 127, Article 103777. <https://doi.org/10.1016/j.compgeo.2020.103777>
2. Feng, J.X., Ni, P.P., & Mei, G.X. (2019). One-dimensional self-weight consolidation with continuous drainage boundary conditions: Solution and application to clay-drain reclamation. *International Journal for Numerical and Analytical Methods in Geomechanics*, 43(8), 1634–1652. <https://doi.org/10.1002/nag.2928>
3. Fredlund, D.G., & Hasan, J.U. (1979). One-dimensional consolidation theory: unsaturated soils. *Canadian Geotechnical Journal*, 16(3), 521–531. <https://doi.org/10.1139/t79-058>
4. Fredlund, D.G., Rahardjo, H., & Fredlund, M.D. (2012). *Unsaturated soil mechanics in engineering practice*. John Wiley & Sons, Inc. <https://doi.org/10.1002/9781118280492>
5. Gibson, R.E., & Shefford, G.C. (1968). The efficiency of horizontal drainage layers for accelerating consolidation of clay embankments. *Géotechnique*, 18(3), 327–335. <https://doi.org/10.1680/geot.1968.18.3.327>
6. Gu, L.L., Wang, Z., Huang, Q., Ye, G.L., & Zhang, F. (2020). Numerical investigation into ground treatment to mitigate the permanent train-induced deformation of pile-raft-soft soil system. *Transportation Geotechnics*, 24, Article 100368. <https://doi.org/10.1016/j.trgeo.2020.100368>
7. He, Q., Yuan, Q., Lang, L., & Cao, J.X. (2025). Implicit difference solution for one-dimensional consolidation of unsaturated soil: Numerical verification and application to soil-cushion system. *Mathematical Geosciences*, 57, 951–976. <https://doi.org/10.1007/s11004-025-10177-6>
8. Lee, S.L., Karunaratne, G.P., Yong, K.Y., & Ganeshan, V. (1987). Layered clay-sand scheme of land reclamation. *Journal of Geotechnical Engineering*, 113(9), 984–995. [https://doi.org/10.1061/\(ASCE\)0733-9410\(1987\)113:9\(984\)](https://doi.org/10.1061/(ASCE)0733-9410(1987)113:9(984))
9. Lei, G.H., Li, Z., & Xu, L.D. (2016). Free-strain solutions for two-dimensional consolidation with sand blankets (in Chinese). *Chinese Journal of Geotechnical Engineering*, 38(2), 193–201. <https://doi.org/10.11779/CJGE201602001>
10. Li, H.P., Chen, Z., Feng, J.X., Meng, Y.H., & Mei, G.X. (2020). Study on position optimization of horizontal drainage sand blanket of double-layer foundation (in Chinese). *Rock and Soil Mechanics*, 41(2), 437–444.
11. Li, L.Z., Qin, A.F., & Jiang, L.H. (2021). Semi-analytical solution for one-dimensional consolidation of a two-layered soil system with unsaturated and saturated conditions. *International Journal for Numerical and Analytical Methods in Geomechanics*, 45(15), 2284–2300. <https://doi.org/10.1002/nag.3266>
12. Li, L.Z., Qin, A.F., Jiang, L.H., & Wang, L. (2022). One-dimensional consolidation of unsaturated-saturated soil system considering pervious or impervious drainage condition induced by time-dependent loading. *Computers and Geotechnics*, 152, Article 105053. <https://doi.org/10.1016/j.compgeo.2022.105053>
13. Meng, Y.H., Chen, Z., Feng, J.X., Li, H.P., & Mei, G.X. (2019). Optimization of one-dimensional foundation with sand blankets under the non-uniform distribution of initial excess pore water pressure (in Chinese). *Rock and Soil Mechanics*, 40(12), 4793–4800. <http://doi.org/10.16285/j.rsm.2018.1899>
14. Mesri, G., & Funk, J.R. (2015). Settlement of the Kansai International Airport Islands. *Journal of Geotechnical and Geoenvironmental Engineering*, 141(2), Article 04014102. [https://doi.org/10.1061/\(ASCE\)GT.1943-5606.0001224](https://doi.org/10.1061/(ASCE)GT.1943-5606.0001224)
15. Moradi, M., Keshavarz, A., & Fazeli, A. (2019). One dimensional consolidation of multi-layered unsaturated soil under partially permeable boundary conditions and time-dependent loading. *Computers and Geotechnics*, 107, 45–54. <https://doi.org/10.1016/j.compgeo.2018.11.020>
16. Morton, K.W., & Mayers, D.F. (2005). *Numerical solution of partial differential equations: An introduction* (2nd ed.). Cambridge University Press, Cambridge, UK.

17. Qin, A.F., Chen, G.J., Tan, Y.W., & Sun, D.A. (2008). Analytical solution to one-dimensional consolidation in unsaturated soils. *Applied Mathematics and Mechanics – English Edition*, 29, 1329–1340. <https://doi.org/10.1007/s10483-008-1008-x>
18. Sharifi, S., & Rashidinia, J. (2016). Numerical solution of hyperbolic telegraph equation by cubic B-spline collocation method. *Applied Mathematics and Computation*, 281, 28–38. <https://doi.org/10.1016/j.amc.2016.01.049>
19. Terzaghi, K. (1943). *Theoretical soil mechanics*. John Wiley and Sons, Inc. <https://doi.org/10.1002/9780470172766>
20. Wang, L., Sun, D.A., Li, L.H., Li, P.C., & Xu, Y.F. (2017). Semi-analytical solutions to one-dimensional consolidation for unsaturated soils with symmetric semi-permeable drainage boundary. *Computers and Geotechnics*, 89, 71–80. <https://doi.org/10.1016/j.compgeo.2017.04.005>
21. Wang, L., Xu, Y.F., Xia, X.H., He, Y.L., & Li, T.Y. (2019). Semi-analytical solutions to two-dimensional plane strain consolidation for unsaturated soils under time-dependent loading. *Computers and Geotechnics*, 109, 144–165. <https://doi.org/10.1016/j.compgeo.2019.01.002>
22. Wu, J., Xi, R., Liang, R., Zong, M., & Wu, W. (2023). One-dimensional nonlinear consolidation for soft clays with continuous drainage boundary considering non-Darcy flow. *Applied Sciences*, 13(6), Article 3724. <https://doi.org/10.3390/app13063724>
23. Yuan, Q., He, Q., Lang, L., & Yang, X.B. (2023). Analytical solution for Fredlund-Hasan unsaturated consolidation using mode superposition method. *International Journal for Numerical and Analytical Methods in Geomechanics*, 47(17), 3234–3247. <https://doi.org/10.1002/nag.3618>
24. Zhou, T., Wang, L., Li, T.Y., Wen, M.J., & Zhou, A.N. (2023). Semi-analytical solutions to the one-dimensional consolidation for double-layered unsaturated ground with a horizontal drainage layer. *Transportation Geotechnics*, 38, Article 100909. <https://doi.org/10.1016/j.trgeo.2022.100909>
25. Zhou, T., Yan, X.L., Wang, L., Zhou, A.N., & Sun, D.A. (2024). Semi-analytical solution for one-dimensional consolidation of a two-layered unsaturated-saturated soil system ground with a horizontal drainage layer. *Computers and Geotechnics*, 169, Article 106196. <https://doi.org/10.1016/j.compgeo.2024.106196>

*Manuscript received September 20, 2024; accepted for publication April 3, 2025;
published online September 27, 2025.*

